THE AMERICAN SOCIETY OF MECHANICAL ENGINEERS
345 E. 47th St., New York, N.Y. 10017

96-GT-133

Numerical Prediction of the Dynamic Behaviour of Turbulent Diffusion Flames

Dieter Bohn, Gregor Deutsch and Uwe Krüger
Institute of Steam and Gas Turbines
Aachen University of Technology
Germany

ABSTRACT

Environmental compatibility requires low emission burners for gas turbine power plants as well as for jet engines. In the past significant progress has been made developing low NO_x and CO burners. Unfortunately these burners often have a more pronounced tendency than conventional burner designs to produce combustion driven oscillations The oscillations may be excited to such an extent that pronounced pulsation may possibly occur; this is associated with a risk of engine failure.

The stability of a burner system can be investigated by means of a stability analysis under the assumption of acoustical behaviour. The problem with all these algorithms is the transfer function of the flame. A new method is presented here to predict the dynamic flame behaviour by means of a full Navier-Stokes-simulation of the complex combustion process. The first step is to get a steady-state solution of a flame configuration. After that a transient simulation follows with a sudden change in the mass flow rate at the flame inlet. The time-dependent answer of the flame to this disturbance is then transformed into the frequency space by a Laplace Transformation. This leads, in turn, to the frequency response representing the dynamic behaviour of the flame.

In principle, this method can be adapted for both diffusion as well as premixed flame systems. However, due to the fact that diffusion flames are more controlled by the mixing process than by the chemical kinetic, the method has first been used for the prediction of the dynamic behaviour of turbulent diffusion flames. The combustion has been modelled by a mixed-is-burnt model. The influence of the turbulence has been taken into account by a modified k-ε-model and the turbulence influences the combustion rate by presumed probability density functions (pdf).

The steady-state as well as the transient results have been compared with experimental data for two different diffusion flame configurations. Although the burner configuration is relatively complex, the steady state results collaborate very well with the experiments for velocity, temperature and species distribution. The most important result is that the heat release which drives the oscillations can be modelled sufficiently accurately. The effect of using different pdf-models has been discussed and the best model has been used for the transient calculations of the dynamic flame behaviour.

The results for the frequency response of the flame are very encouraging. The principal behaviour of the flame - higher order time element with a delay time - can be predicted with sufficient precision. In addition, the qualitative results collaborate fairly well with the experiments.

NOMENCLATURE

C	general constant
c_p	specific heat capacity
F	frequency response
F	fuel
f	mixture fraction
g	variance of mixture fraction
H_u	net calorific power
h	unit function response
h	enthalpy
j	complex variable
k	turbulent kinetic energy
M	molecular weight
$\dot{m}$	mass flow rate
$\Delta\dot{m}$	jump function
O	oxidant
P	product
p	pressure
p	probability density function
$\dot{q}$	transient heat release
R	gas constant

Presented at the International Gas Turbine and Aeroengine Congress & Exhibition
Birmingham, UK — June 10-13, 1996
This paper has been accepted for publication in the Transactions of the ASME
Discussion of it will be accepted at ASME Headquarters until September 30, 1996

t	time
T	temperature
Tu	turbulence intensity
$\bar{v}$	velocity vector
u,v,w	axial, radial and circumferential velocity component
x,r,ϕ	axial, radial and circumferential coordinate
α	stoichiometric oxidant mass
ε	turbulent dissipation rate
μ	viscosity
ρ	density
ξ	mass fraction
ψ	mole fraction
φ	phase angle
ϕ	equivalence ratio
ω	angular frequency

SUBSCRIPTS

F	fuel
fl	flame
O	oxidant
P	product
st	stoichiometric
t	total
T	turbulent
	average value

INTRODUCTION

Due to the need for environmental compatibility, combustion is a very important field of research in gas turbine development. In the past significant progress has been made developing low NO_x and CO burners. In addition, the power output of heavy duty gas turbines has increased significantly, with the result that the thermal power of the combustion chamber is greater. Unfortunately these advanced burners and combustion chambers often have a more pronounced tendency to produce combustion driven oscillations than conventional burner designs. The oscillations may be excited to such an extent that pronounced pulsation may possibly occur; this is associated with a risk of engine failure. They can lead to higher levels of pollution and result in very high noise emissions. Therefore, there is an urgent need to develop a design tool for the prediction of these instabilities. It is important to understand that they are not sympathetic vibrations, so variations of geometry will not prevent them automatically [Baade (1)].

The stability of a burner system can be investigated by means of a stability analysis under the assumption of acoustical behaviour. At the Institute of Steam and Gas Turbines, RWTH Aachen, an acoustical model has been developed to predict the stability range of a combustor [Bohn and Deuker (2), Deuker (3)]. The combustor is therefore split up into several units, as shown in principle in figure 1. The whole combustor works as a feedback system leading to self induced oscillation under special assumptions. This model was successfully tested and verified with experimental data taken from a test combustor. For further details see [Bohn and Deuker (2)]. However, in order to predict the instabilities of real gas turbine burners, a thorough understanding of the dynamic behaviour of the flame which works as an

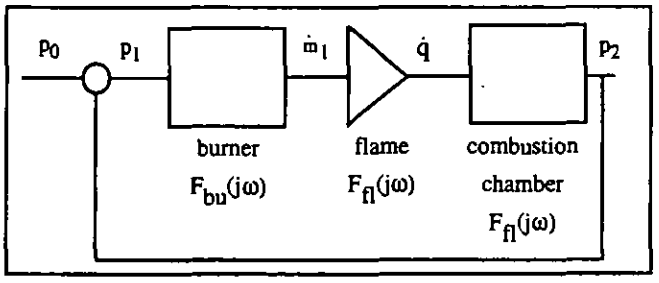

FIG. 1: Oscillating Circuit of a Combustor System

amplifier in this oscillating circuit is required.

Some experimental work in this area can be mentioned. [Lenz (4)] and [Lang (5)] have investigated the dynamic behaviour of turbulent premixed flames. [Matsui (15) and Sugimoto and Matsui (16)] did further experimental work on laminar premixed flames. [Priesmeier (6)] did experiments on the dynamic behaviour of diffusion flame systems. All authors deduced that the frequency response of flames can be described as a higher order time element with a delay time. The behaviour of the flame depends strongly on the geometry of the burner, the type of flame, the equivalence ratio and the thermal power.

Some theoretical work has been done by [Merk (7)], [Becker and Günther (8)], [Lenz (4)] and [Bohn and Deuker (2)]. In combination with the experimental work mentioned above, these analytical works are very helpful for describing the principles of dynamic flame behaviour. In the case of practical flames, which are characterized by complex geometries, and highly turbulent fluid flows, however, these analyses are not precise enough because many assumptions have to be postulated in order to derive the frequency response of flames.

In this paper a new method is used - first described in [Bohn and Krüger (9)] - which derives the frequency response by means of a transient numerical simulation of the complex combustion process.

DERIVATION OF THE FLAME FREQUENCY RESPONSE

The principal method used to calculate the frequency response of a flame by numerical simulation of the combustion process is sketched in figure 2. First, the steady-state combustion process of a given configuration has to be calculated. After that, transient calculations are carried out which give the time-dependent unit function response of the flame (h(t)) to a sudden increase in the

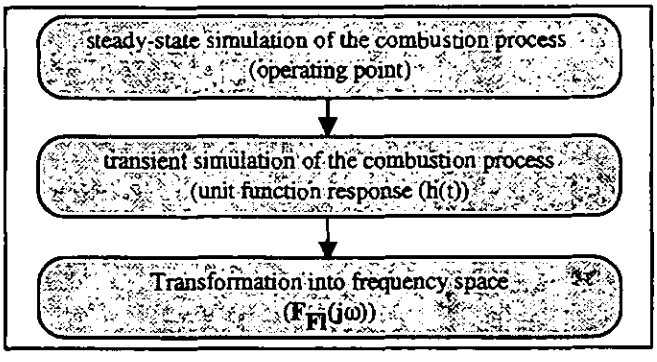

FIG. 2: NUMERICAL SIMULATION OF THE DYNAMICAL BEHAVIOUR

mass flow rate of air at the burner inlet:

$$h(t) \equiv \frac{\Delta \dot{q}_{flame}}{\Delta \dot{m}} \tag{1}$$

This response is then transferred into frequency space by a Laplace Transformation to obtain the frequency response of the flame $F_{fl}(j\omega)$:

$$F_{fl}(j\omega) = j\omega \int_0^{\infty} h(t) \cdot e^{-j\omega t} dt \tag{2}$$

In the case of diffusion flames it is expedient to define the ratio of the transient heat release of the flame to the mass flow jump of air - mass flow rate of air is much larger than that of fuel - at the burner inlet as the characteristic value for the dynamic behaviour of the flame. The advantage of this definition is that this ratio is independent of the computational domain. The definition (1) is compatible with that used by [Priesmeier (6)].

Due to the thermal inertia of the system, this procedure cannot be used for experimental investigations. Therefore the flame is perturbed by harmonic disturbance, i. e. a sinusoidal variation of the inlet mass flow. In order to obtain the frequency response, many discrete frequencies have to be investigated; this means that a lot of effort has to be invested in experimental work. These two different methods for obtaining the frequency responses of a dynamic system are absolutely equivalent under the assumption of linear systems, which is really true for the beginning of self-induced oscillations [Baade (1)].

NUMERICAL PROCEDURE

BASIC EQUATIONS

Under the assumption of fast chemistry - which means that the turbulent mixing of fuel and oxidant dominates the combustion process - the combustion chemistry can be given by only one simple reaction equation:

$$\underbrace{1\,\mathrm{kg\,F}}_{\text{Fuel}} + \underbrace{\alpha\,\mathrm{kg\,O}}_{\text{Oxidant}} \rightarrow \underbrace{(1+\alpha)\,\mathrm{kg\,P}}_{\text{Product}} \tag{3}$$

Neglecting the chemical kinetic effects fuel is burnt infinitesimal fast, consuming all available oxidant. This model which is often used for diffusion flame systems is called the mixed-is-burnt-model.

Then, the entire combustion process of a turbulent diffusion flame can be described by the Favre averaged transient and compressible Navier-Stokes-equations (4-6), the equations for the turbulence quantities k (7) and ε (8), the mixture fraction f (9) and the variance of the mixture fraction g (10):

$$\frac{\partial \rho}{\partial t} + \nabla \cdot (\rho \bar{v}) = 0 \tag{4}$$

$$\frac{\partial \rho \bar{v}}{\partial t} + \nabla \cdot (\rho \bar{v} \times \bar{v} - (\mu + \mu_T)\nabla \bar{v}) = -\nabla (p + \frac{2}{3}\rho k) + \nabla \cdot \left((\mu + \mu_T)(\nabla \bar{v})^T\right) \tag{5}$$

$$\frac{\partial \rho h_t}{\partial t} + \nabla \cdot \left(\rho \bar{v} h_t - \left(\frac{\lambda}{c_p} + \frac{\mu_T}{\sigma_{Th}}\right)\nabla h_t\right) = \frac{\partial p}{\partial t} \tag{6}$$

$$\frac{\partial \rho k}{\partial t} + \nabla \cdot \left(\rho \bar{v} k - \left(\mu + \frac{\mu_T}{\sigma_{Tk}}\right)\nabla k\right) = P - \rho\varepsilon \tag{7}$$

$$\frac{\partial \rho \varepsilon}{\partial t} + \nabla \cdot \left(\rho \bar{v} \varepsilon - \left(\mu + \frac{\mu_T}{\sigma_{T\varepsilon}}\right)\nabla \varepsilon\right) = C_1 \frac{\varepsilon}{k} P - C_2 \rho \frac{\varepsilon^2}{k} \tag{8}$$

$$\frac{\partial \rho f}{\partial t} + \nabla \cdot \left(\rho \bar{v} f - \left(\frac{\mu}{\sigma_f} + \frac{\mu_T}{\sigma_{Tf}}\right)\nabla f\right) = 0 \tag{9}$$

$$\frac{\partial \rho g}{\partial t} + \nabla \cdot \left(\rho \bar{v} g - \left(\frac{\mu}{\sigma_g} + \frac{\mu_T}{\sigma_{Tg}}\right)\nabla g\right) = C_{g1} \frac{\mu_T}{\sigma_T} (\nabla f)^2 - C_{g2} \rho \frac{\varepsilon}{k} g \tag{10}$$

P is the production term of turbulence energy and turbulence dissipation due to shear forces. There are several empirical constants appearing in both the turbulence and the combustion model. In table 1, the used values of these constants are listed; however these values are all known as standard values, apart from C_1 which appears in the epsilon equation (8).

C_1	C_2	C_{g1}	C_{g2}	σ_{Th}	σ_{Tk}	$\sigma_{T\varepsilon}$	σ_f	σ_{Tf}	σ_g	σ_{Tg}
(1.44)1.6	1.92	2.22	2	0.9	1	$\frac{0.4187^2}{(C_2 - C_1)\sqrt{0.09}}$ 0.7		0.9	0.7	0.9

TAB. 1: CONSTANTS OF THE NUMERICAL SCHEME

This number has been changed from 1.44 to 1.6 which is often used for problems with free jets. As shown in table 1 this has also consequences on the turbulent Prandtl number $\sigma_{T\varepsilon}$ of the epsilon equation. The effects of this change will be discussed later on. The influence of turbulence on the mixture fraction - representing the combustion progress - is taken into account by presumed probability density functions (see figure 3). Three different forms have been used and tested:

Single Delta Function (δ-pdf):

$$p(f) = \delta(f - \bar{f}) \tag{11}$$

Double Delta Function (2δ-pdf):

$$p(f) = \begin{cases} \frac{1}{2}\delta\left(f - \left(\bar{f} + \sqrt{\bar{g}}\right)\right) + \frac{1}{2}\delta\left(f - \left(\bar{f} - \sqrt{\bar{g}}\right)\right) & \text{if } \left(\bar{g} \le (1-\bar{f})^2\right) \wedge \left(\bar{g} \le \bar{f}^2\right) \\ \frac{\bar{g}}{\bar{f}^2 + \bar{g}}\delta(f) + \frac{\bar{f}^2}{\bar{f}^2 + \bar{g}}\delta\left(f - \left(\bar{f} + \frac{\bar{g}}{\bar{f}}\right)\right) & \text{if } \bar{f}^2 \le \bar{g} \le \bar{f}(1-\bar{f}) \\ \frac{\bar{g}}{(1-\bar{f})^2 + \bar{g}}\delta(f-1) + \frac{(1-\bar{f})^2}{(1-\bar{f})^2 + \bar{g}}\delta\left(f - \left(\bar{f} - \frac{\bar{g}}{(1-\bar{f})}\right)\right) & \text{if } (1-\bar{f})^2 \le \bar{g} \le \bar{f}(1-\bar{f}) \end{cases} \tag{12}$$

Beta Function (β-pdf):

$$p(f) = \frac{\Gamma(a+b)}{\Gamma(a)\Gamma(b)} f^{a-1}(1-f)^{b-1} \tag{13}$$

where:

$$a = \frac{\bar{f}}{\bar{g}}\left(\bar{f}(1-\bar{f}) - \bar{g}\right) \quad \text{and} \quad b = \frac{(1-\bar{f})}{\bar{g}}\left(\bar{f}(1-\bar{f}) - \bar{g}\right) \tag{13 a}$$

Then, the mass fractions of fuel, oxidant and product are given by:

$$\xi_F = \int_0^1 \max\left(\frac{f - f_\mu}{1 - f_\mu}, 0\right) p(f)\,df \tag{14}$$

$$\xi_O = \int_0^1 \max\left(1 - \frac{f}{f_\mu}, 0\right) p(f)\,df \tag{15}$$

$$\xi_P = 1 - \xi_F - \xi_O \tag{16}$$

The stoichiometric mixture fraction f_{st} depends on the fuel used - here all investigations are carried out with methane (α=17.2), leading to a value of f_{st} = 0.055 - and is defined as:

$$f_{st} = \frac{1}{1+\alpha} \tag{17}$$

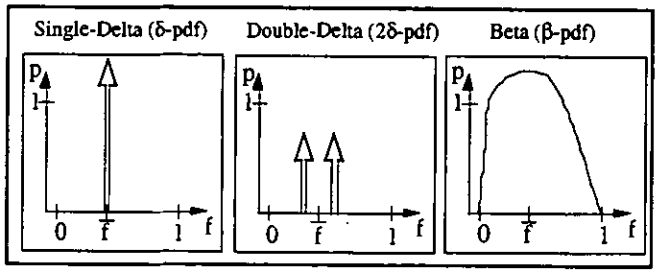

FIG. 3: DIFFERENT PROBABILITY DENSITY FUNCTIONS (PDFS9)

The set of 9 coupled differential equations (4 - 10) is closed by the equation of state for ideal gases (18) and the constitutive equation for ideal gases (19):

$$\rho = \frac{p}{RT} \tag{18}$$

$$h = \int_{T_{ref}}^{T} c_p(\xi_i, T)dT + \xi_F H_u \tag{19}$$

In equation 19, the second term represents the heat release as a result of the combustion process, where H_u is the net calorific value.

Finally, for ideal gas mixtures - here the mixture consists of fuel (ξ_F), oxidant (ξ_O) and product (ξ_P) - the specific gas constant and the specific heat capacity are defined as:

$$R = \frac{\Re}{M} \text{ where } \frac{1}{M} = \sum_{i=1}^{n} \frac{\xi_i}{M_i} \tag{20}$$

$$c_p(\xi_i, T) = \sum_{i=1}^{n} \xi_i c_{p,i}(T) \tag{21}$$

SOLUTION METHOD

A fully implicit finite-volume scheme has been used for solving the coupled equations (4)-(10). The SIMPLEC pressure-correction algorithm [Van Doormal and Raithby (10)] is adapted on a non-staggered grid, while avoiding the chequerboard oscillations by using the improved Rhie-Chow interpolation method [Rhie (11) and Rhie and Chow (12)]. For diffusion terms, a central differencing scheme is used, while advection terms are discretised by upwind differencing. A fully backward difference time stepping procedure is employed. Therefore, the time step is not bound to CFL stability restrictions in principle: this is a very important feature for numerical investigations of transient combustion phenomena.

BURNER GEOMETRIES

Two different burner geometries have been used for testing the steady-state as well as the transient flow with and without combustion included. A cutout of the two burner configurations is shown in figure 4 - for clarity, only the head ends of the combustion chambers where the reactants are introduced and the flame is stabilized are plotted. The main difference between these two burners is the stabilizing mechanism. The flame of burner 1 is stabilized by a baffle plate at the burner exit. Methane (fuel) is flowing through the inner duct, while the air (oxidant) is flowing through the outer one. The acceleration induced by the baffle plate leads to a radial component at the burner exit and two antispin vortices downstream of the exit. This vortices stabilize the flame due to the low flow velocities which have to be on the order of the burning velocity of the flame. Burner 2 is characterized by a different stabilizing method. A very small pilot flame is produced directly at the burner exit. Therefore, between the inner fuel jet and the outer air jet, there is a third nozzle through which pure oxygen O_2 is flowing. The burner can therefore be referred to as O_2-stabilized. Oxygen is used for the pilot flames instead of air due to the fact that O_2 flames have a higher adiabatic flame temperature.

Both burners have been developed and experimentally investigated at the University of Karlsruhe [Priesmeier (6) and Prade (13)]. For burner 1 steady-state investigations for the cold flow configuration as well as for the combustion configuration are available. The velocities were measured by a LDV-measurement technique, concentration profils were measured by watercooled probes and the temperatures were obtained by Pt/Pt-Ro thermocouples. Experimental results of the dynamic flame behaviour are available only for burner 2, for which the transient heat release is measured by OH-radiant technique.

GRID AND BOUNDARY CONDITIONS

In figure 5 a cut of the structured computational grids for the two burners are shown. Using the multiblock technique it is possible to take into account not only the domain downstream of the burner exit but also the internal flow of the burner itself. This is more general as one can give boundary conditions at the burner inlet and no information is needed about the very important - and

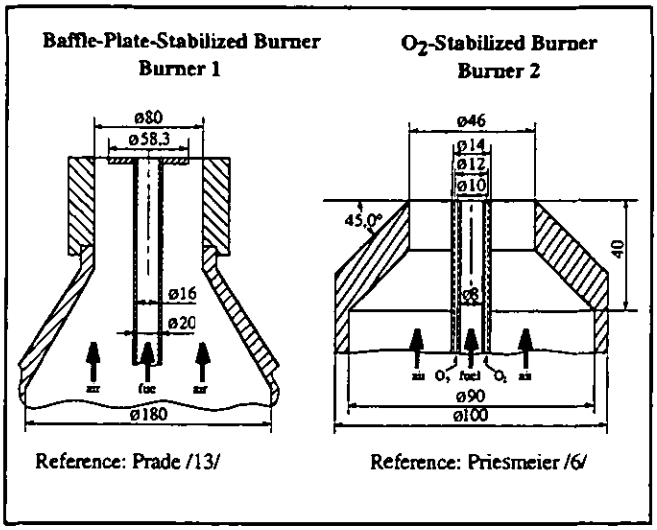

FIG. 4: BURNER CONFIGURATIONS

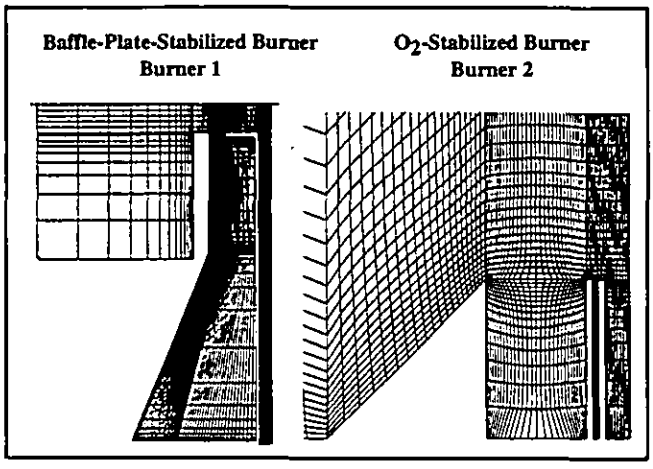

FIG. 5: COMPUTATIONAL GRIDS

in most cases unknown - flow conditions at the burner exit. This is an essential cause of the very complex flow situation especially in the case of burner 1.

The boundary conditions for the steady-state calculations are shown in figure 6. For burner 1 these values lead to an air mass flow rate of 32.4 g/s and to a fuel mass flow rate of 3.14 g/s (equivalence ratio ϕ=1.66). For burner 2 the air mass flow rate is 21.2 g/s, the fuel mass flow rate is 1.18 g/s and the oxygen mass flow rate of the pilot flame is 0.056 g/s. Neglecting the oxygen flame this results in an equivalence ratio of ϕ=0.95. For the transient calculations of burner 2, the mass flow rate of air is increased by 20% of the steady state value.

RESULTS

Before starting the transient calculations, two main topics have to be investigated. Firstly, the flow has turbulent character, with the result that the turbulence modelling has to be evaluated. To

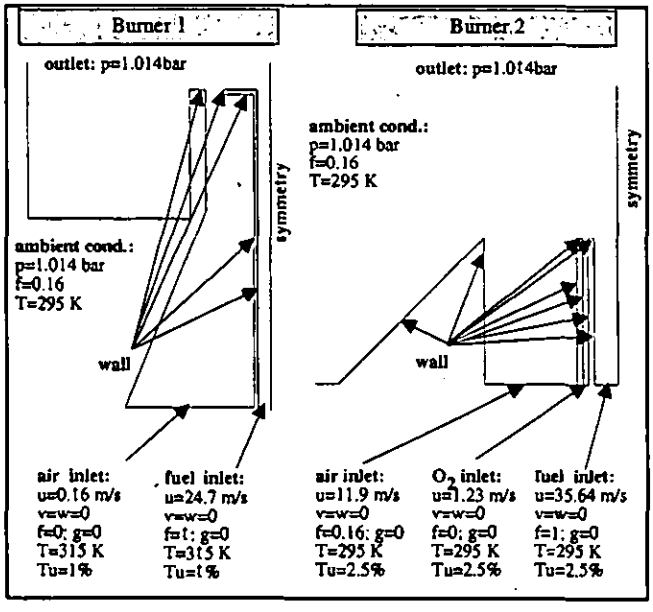

FIG. 6: BOUNDARY CONDITIONS

separate the effects, it is worthwhile to validate this on cold flow configurations. This has been done for both burners. However, due to the fact that burner 1 has the more complex geometry, results will be presented for this configuration only. Secondly, the combustion process itself and the interaction with turbulent mixing has to be evaluated. The temperature distribution in particular is of great interest because this is essential for the transient heat release during the combustion process following a sudden jump in the mass flow rate at the burner exit.

COLD FLOW

The principal flow pattern of the baffle stabilized burner (burner 1) can be illustrated by figure 7 in which the velocity vectors are shown near the burner exit. In principle, the numerical results collaborate well with the measured one. The two vortices of the return flow can be clearly identified. These vortices are very important for the stabilization mechanism of this burner. Apart from the advantage that no information about the boundary conditions at the burner exit is needed, the fact that such important details as the separation of the air jet at the baffle plate can be predicted makes it straightforward to take into account the internal flow of the burner.

In order to evaluate the used standard k-ε model, the quantitative results of the numerical simulation of the isotherm flow are presented in figure 8. The axial velocity u and the concentration of methane Ψ_{Fuel} are plotted against the dimensionless radius - the radius is normalized by the radius of the fuel nozzle r_0 - for two different axial positions 24 mm (x/r_0=3) and 60 mm (r/r_0=7.5) downstream of the burner nozzle. Two different values of the C_1 parameter of the ε-equation (egn. 8) are used: the standard value of 1.44 and a value of 1.6, which is often used for free jet configurations. It is clearly shown that for both axial positions, the calculations with C_1=1.6 match the meaurements almost perfectly. In particular, the most important region in which flow return between fuel and air jet occurs is calculated extremely precisely. This is also true for the prediction of the fuel species which is characterized by the turbulent mixing process. The results discussed above show that the standard k-ε-turbulence model, with the correction of the parameter C_1 in the ε-equation,

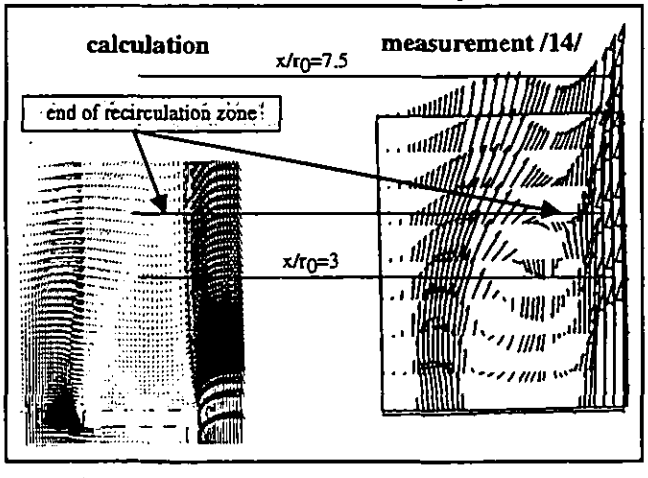

FIG. 7: VELOCITY-VECTORPLOT: COMPARISON BETWEEN MEASUREMENT AND CALCULATION

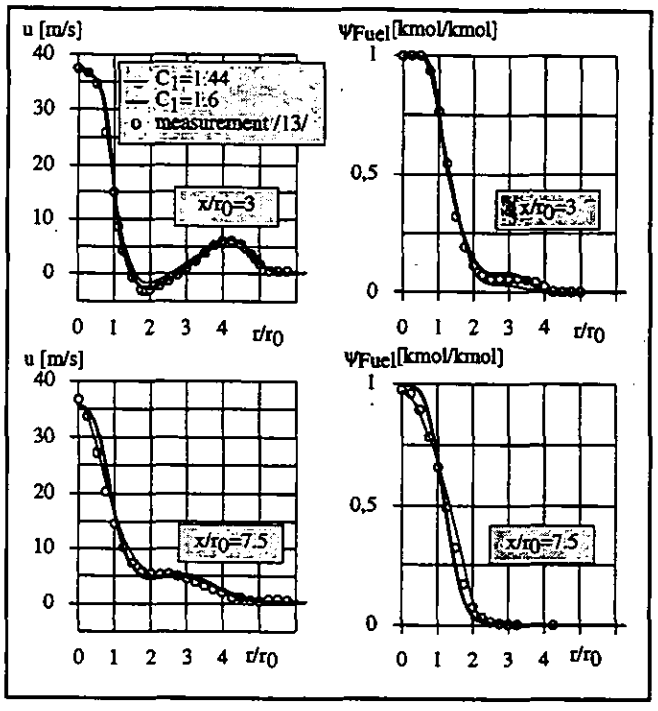

FIG. 8: VALIDATION OF TURBULENCE MODEL

is suitable for the prediction of the flow pattern in a multi-jet, multi-component diffusion flame system.

STEADY-STATE-COMBUSTION

The steady-state combustion process for the turbulent diffusion flame system has been calculated for the purpose of validating the combustion model and in particular, the probability density function used. In addition, the calculation serves to obtain a steady-state operating point to start the transient calculation for getting the frequency response of the flame.

In figure 9 the distribution of temperature and the mass fraction of the fuel is shown for the entire burner system of burner 1. The reaction zone can be clearly detected by the strong temperature gradients. As is typical for diffusion flames, the reaction zone is displaced on the lean air side. The influence of the radial component of velocity at the air exit of the burner on the distribution is given by the s-shaped reaction zone.

To evaluate the quality of the numerical results and to decide which pdf (see eqn. 11-13) to choose for predicting the heat release in figure 10, a comparison between measurements [Leuckel (14)] and three calculations with different pdfs is shown for four different axial positions (16 mm (x/r_0=2), 32 mm (x/r_0=4), 54 mm (x/r_0)=6.8) and 64 mm (x/r_0=8) downstream of the burner exit). The single delta function (eqn. 11) is not suitable for predicting the temperature distribution correctly. Due to the nature of this pdf, the effects of turbulence on the mixture fraction f are neglected. Consequently, the predicted temperatures are too high compared to reality. The maximum temperature of 2200 K is almost equal to the adiabatic flame temperature of methane. This result shows how important it is to consider the interaction between turbulence and combustion, especially for gas turbine combustors.

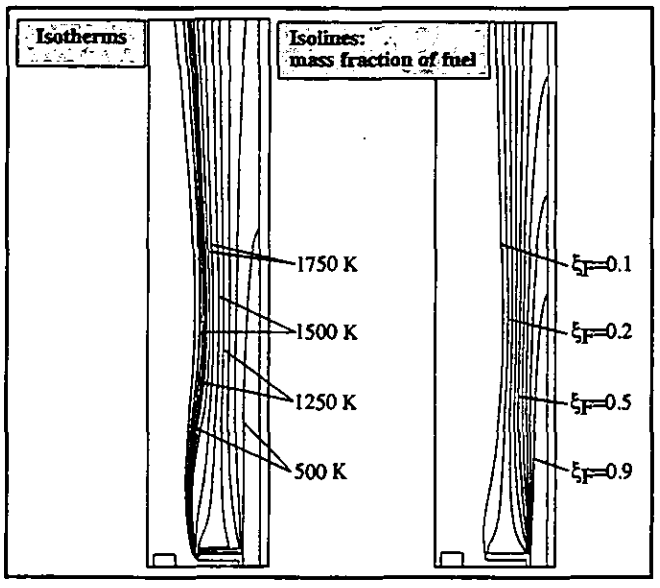

FIG.9: BAFFLE-PLATE-STABILIZED BURNER: STEADY-STATE-CALCULATION

Near the burner exit, there is no significant difference between the double delta function (eqn. 12) and the beta function (eqn. 13). This changes further downstream of the burner. For some reason, the double delta function tends to underestimate the temperature and shows two similar peaks one on the lean side and one on the rich side of the flame. These results demonstrate that the beta-pdf gives the best results for the important temperature distribution. The calculated temperature only overestimates measurements

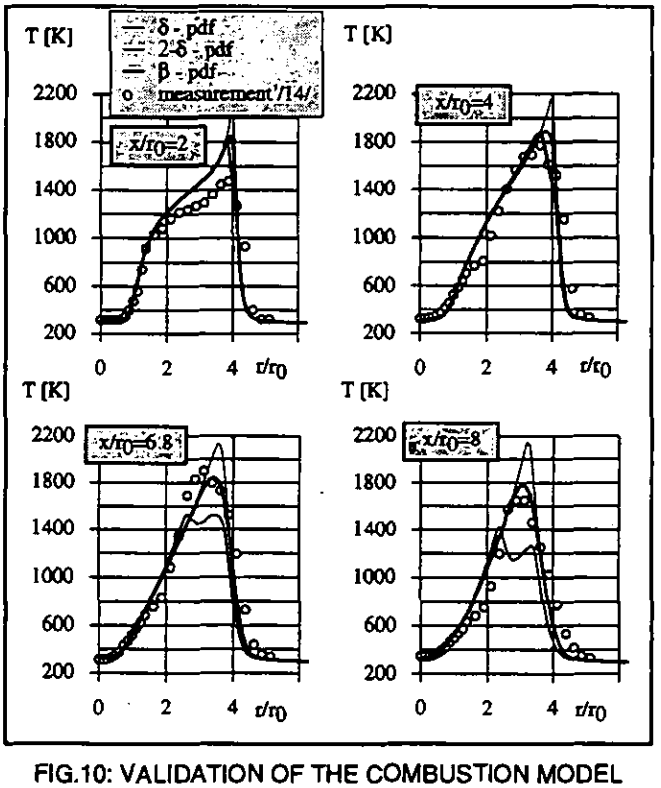

FIG.10: VALIDATION OF THE COMBUSTION MODEL

very near to the burner exit. This can be explained on the one hand side by the fact that chemical kinetic effects are neglected by the mixed is burnt model and on the other hand side by the temperature measurement which seems to have a slight tendency to underestimate temperature in the very rich zone of the flame.

The steady-state operation point for the O_2-stabilized burner has been calculated by the turbulence and combustion model as discussed in detail above. The temperature and fuel distribution is shown in figure 11. Some modification of the model has been introduced due to the fact that three jets - fuel, air and O_2 - exist. The small pilot flame is also shown in figure 11. The O_2-methane flame produces very high temperatures compared to the main air-methane flame. As proven by the experiments of [Priesmeier (6)], this pilot flame has no significant influence on the dynamic behaviour of the main flame, but instead stabilizes the flame at the burner exit. It is important to mention that only 1/4 of the entire computational domain is shown in axial direction in this figure. Because of the lean configuration all fuel is burnt inside the complete computational domain.

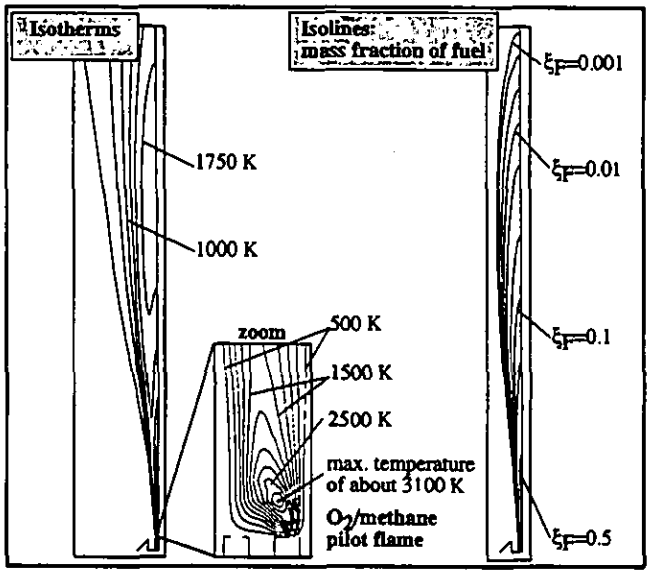

FIG.11: O_2-STABILIZED BURNER: STEADY-STATE CALCULATION

TRANSIENT FLAME MODELLING

Transient calculations have been performed for burner 2 in order to obtain the unit function response which can be transferred into frequency space by a Laplace Transformation. Therefore, after the converged steady-state solution is obtained, the mass flow rate at the air inlet has been increased by 20% of the operation point mass flow rate. One attempt has also been made to check the linearity of the system with 5% jump height, but the result - the unit function response - shows no significant difference. Thus, it can be concluded that linearity of the system exists, at least for a jump height up to 20%. Figure 12 displays the unit function response h(t) calculated which is defined as the ratio of the heat release to the mass flow jump at the burner inlet (eqn. 1). For a time of zero, h(t) is zero by definition - if we remember

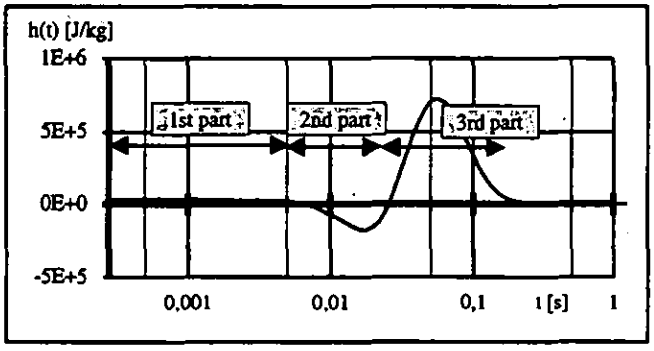

FIG.12: UNIT FUNCTION OF THE TURBULENT DIFFUSION FLAME

that $\dot{q}_{flame}$ is only the difference between the transient heat release and the steady-state heat release of the operation point. For times going to infinity, h(t) is again zero which is due to the fact that all methane is burnt inside the computational domain. The unit function response can be divided into three parts, as is shown in figure 12. In part 1, the time is in the order of the length of the computational domain (2 m) divided by the sound velocity, which differs between 350.0 m/s for the unburnt and 850.0 m/s for the hottest zones of the exhaust gas. In this part there is a short period of low amplification (from t=0 s to t=6 ms). This can be explained by the transportation of the disturbance with sound velocity. After this period the combustion process is disturbed; this leads to a lower heat release than the steady-state heat release. In the 3rd part, the combustion process is strongly amplified leading to higher heat release. After 0.5 s, the steady-state-condition is reached again and the flame produces the same heat release as before. Integrating h(t) over the time, there is much more heat produced. This can be explained by looking at the shape of the flame. After increasing the air mass flow, the mixing process is improved resulting in a shorter flame than the flame before the jump. This means that less unburnt methane is stored and the difference must have been burnt, thus producing heat.

The third part is most significant for the dynamic behaviour of the flame; this can be clearly seen by looking at the frequency response shown in figure 13 in Bode's diagram. In this figure, the experimental results [Priesmeier (6)] can be compared to the numerical calculation of the dynamic behaviour. The magnitude of the frequency response is normalized by the magnitude for low frequencies [Priesmeier (6)]. The principle behaviour of the flame, which is characterized by a higher order time element with a delay time, can be described sufficiently accurately. The magnitude of the frequency response shows high values up to an angular frequency of about 100 1/s. After that there is only a small decrease in the magnitude up to an angular frequency of about 400 1/s which can be identified as the sharp cutoff. This means that, in principle, this turbulent diffusion flame can amplify self-induced oscillations over a wide angular-frequency range. The comparison between the magnitude of the frequency response calculated with the measured one shows fairly good agreement. Some discrepancies of the phase angle between measurement and calculation have to be mentioned. Up to an angular frequency of 250 1/s there exists a constant phase shift of -180° between the measurement and the calculation. This is corresponding to a sign

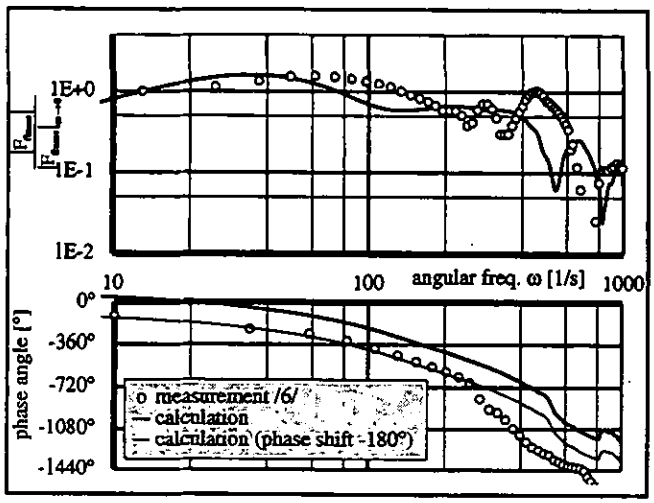

FIG.13: FLAME FREQUENCY RESPONSE

change in the frequency response, which can perhaps be explained by different definitions of the normalization. In any case, the principal behaviour of the phase of the frequency response can be predicted perfectly. The flame shows the characteristics of a perfect delay time element up to an angular frequency of 500 1/s. For higher frequencies the phase angle decreases faster because part 2 of the unit function response becomes dominant. This behaviour has also been measured by [Priesmeier (6)] but the significant angular frequency is smaller (250 1/s). This can be explained due to the fact that kinetic effects are neglected, the flame reacts faster to a disturbance near the burner exit than in reality. To summarize: For low angular frequencies the dynamic behaviour of the turbulent diffusion flame can be described almost perfectly with the mixed is burnt model used. For higher angular frequencies - corresponding to the region near the burner exit - the influence of chemical kinetics becomes more important. Therefore, future work should concentrate on this influence in combination with turbulence transport mechanisms.

Nevertheless, the results are very encouraging. Flame frequency responses are the most important factor in investigations on self-induced combustion-driven oscillations. The results show that the numerical mechanism discussed above is suitable for predicting the dynamic behaviour of such complex flame configurations. In addition, with experimental work, the principal influences of changing burner configurations, combustion parameters etc. can now be discussed much more easily.

All results were obtained on an HP715 workstation. Almost 30% of computer time was needed to calculate the steady-state operation point. Having the experience with this model it is now possible to obtain a freqeuency response of a turbulent diffusion flame in less than one month using modern state of the art workstation hardware.

SUMMARY AND CONCLUSION

A new method has been presented for the numerical prediction of the dynamic behaviour of flames. Frequency responses which describe this behaviour are the most important element of investigations on self-induced combustion-driven osciallations. Due to a reliable operation of a gas turbine, these oscillations must be provided.

To obtain the frequency response, numerical simulation - using a 3-D Navier-Stokes-Code - of the steady-state-operation point is performed, followed by a transient simulation of the combustion process following a sudden increase in the mass flow rate at the burner inlet. This simulation leads to the unit function response which can be transferred into frequency space by a Laplace-Transformation. The method which, in principle, is suitable for both premixed and diffusion flame systems has first been adapted for turbulent diffusion flames.

To evaluate the turbulence and the combustion models and to obtain the steady-state operation point, simulations of the cold and hot steady-state flow of two different diffusion flame systems were initially performed. The results can be summarized as follows:

1. The standard k-ε-turbulence model is suitable for these systems with a well-known correction of the production term in the dissipation equation. The complex flow configuration including the internal flow inside the burner can be predicted extremely precisely.
2. Using the beta-pdf to take into account turbulence effects on the combustion process, the important heat release can be predicted sufficiently accurately. There is only one region where the temperature is overpredicted, i. e. very near to the burner exit. This can be explained using the mixed-is-burnt-model, which neglects chemical kinetics.

After a sudden jump in the air mass flow rate at the inlet, transient numerical simulation generates the unit function response of the flame. The important characteristics of the dynamic behaviour of the flame can be discussed:

1. Up to a delay time of 5 ms only low amplification exists.
2. After a period in which the combustion process is disturbed - less heat is released compared to the steady-state operation point - high amplification follows. This amplification starts after 0.02 s.
3. After 0.5 s the steady-state operation point is reached again.
4. Integrated over time, more heat is released due to the fact that the flame is shorter after the jump, leading to less fuel stored. The difference must have been burnt during the time period.

The frequency response is obtained by a Laplace Transformation of the unit function response. It can be compared with measurements of this diffusion flame system. It can be concluded that:

1. The principal behaviour of the flame collaborates well with the measurements.
2. Due to the high values of the frequency response, the possibility of amplification of self-induced combustion driven oscillations exists.
3. The phase angle shows the typical trend of an element with a delay time. Compared to the measurements the phase angle correlates almost perfectly up to a special angular frequency. After that the predicted delay time is too small. This can again be explained by the fact that the chemical kinetics are neglected.

Nevertheless, the results show the feasibility of the procedure and help to clarify the dynamic flame behaviour in much more

detail. Future work should also concentrate on the influence of chemical kinetics on diffusion flames, which are mainly controlled by the turbulent mixing process. A second very important aspect is the influence of high pressue on the dynamic flame behaviour which is typical for gas turbine applications.

ACKNOWLEGEMENT

The authors would like to thank the "Deutsche Forschungsgemeinschaft" for sponsoring this work by the Graduiertenkolleg "Turbulenz und Verbrennung" at the RWTH Aachen.

REFERENCES

1 **Baade, P.K.** "Selbsterregte Schwingungen in Gasbrennern, Klima Kälte Ingenieur, 1974

2 **Bohn, D.; Deuker, E.** "An Acoustical Model to Predict Combustion Driven Oscillations", 20th International Congress on Combustion Engines (CIMAC), London 1993

3 **Deuker, E.** "Ein Beitrag zur Vorausberechnung des akustischen Stabilitätsverhaltens von Gasturbinenbrennkammern mittels theoretischer und experimenteller Analyse von Brennkammerschwingungen, PhD Thesis, RWTH Aachen, Germany 1995

4 **Lenz, W.** "Die dynamischen Eigenschaften von Flammen und ihr Einfluß auf die Entstehung selbsterregter Brennkammer-schwingungen", PhD Thesis, Uni Karlsruhe (T.H.), Germany, 1980

5 **Lang, W.** "Dynamik und Stabilität selbsterregter Verbrennungs-schwingungen beim Auftreten mehrerer Frequenzen. Ein erweitertes Stabilitätskriterium" PhD Thesis, TU München, Germany, 1986

6 **Priesmeier, U.** "Das dynamische Verhalten von Axialstrahl-Diffusionsflammen und dessen Bedeutung für selbsterregte Brennkammerschwingungen", PhD Thesis, Uni Karlsruhe (T.H.), Germany, 1987

7 **Merk, H. J.** "An Analysis of Unstable Combustion of Premixed Gases", Sixth Symposium (International) on Combustion, 1956

8 **Becker, R.; Günther, R.** "Niederfrequente nichtakustische Druckschwingungen in Brennkammern", Chemie-Ing.-Techn., 1973

9 **Bohn, D.; Krüger, U.** "Experimental and Theoretical Investigations on the Dynmaic Behaviour of Flames Typical Used in Gas Turbine Combustors", Proceedings of the 2nd Summer Conference `Numerical Modelling in Continuum Mechanics', Prague, 1994

10 **Van Dormal, J. P.; Raithby, G. D.** "Enhancements of the SIMPLE method for predicting incompressible flows", Numer. Heat Transfer, 7, 1984, pp 147 - 163

11 **Rhie, C. M.** "A numerical study of the flow past an isolated airfoil with separation, PhD Thesis, Uni of Illinois at Urbana-Champaign, 1981

12 **Rhie, C. M., Chow, W.L.** "Numerical study of the turbulent flow past an airfoil with trailing edge separation", AIAA J1, 21, 1983, pp 1527 - 1532

13 **Prade, B.** "Experimentelle und theoretische Untersuchung zum Abblaseverhalten von turbulenten Stauscheibendiffusionsflammen"; PhD Thesis, Uni Karlsruhe (T.H.), Germany, 1993

14 **Leuckel, W.** "SFB 169 - Hochbelastete Brennräume - stationäre Gleichdruckverbrennung", Uni Karlsruhe (T.H.), Germany

15 **Matsui, Y.** "An Experimental Study on Pyro-Acoustic Amplification of Premixed Laminar Flames", Combustion and Flame 43, 1981, pp 199-2009

16 **Sugimoto. T. and Matsui, Y.** "An Experimental Study on the Dynamic Behavior of Premixed Laminar Flames", Nineteenth Symposium (International) on Combustion/The Combustion Institute, 1982, pp 245-250